IEEE Access
Multidisciplinary | Rapid Review | Open Access Journal

Received 1 October 2022, accepted 17 October 2022, date of publication 25 October 2022, date of current version 2 November 2022.

Digital Object Identifier 10.1109/ACCESS.2022.3216574

RESEARCH ARTICLE

LSTM-Autoencoder Deep Learning Technique for PAPR Reduction in Visible Light Communication

ABDELFATAH MOHAMED[1], ADLY S. TAG ELDIEN[1], MOSTAFA M. FOUDA[2], (Senior Member, IEEE), AND REHAM S. SAAD[1]

[1]Department of Electrical Engineering, Faculty of Engineering at Shoubra, Benha University, Cairo 11672, Egypt
[2]Department of Electrical and Computer Engineering, College of Science and Engineering, Idaho State University, Pocatello, ID 83209, USA

Corresponding author: Abdelfatah Mohamed (abdelfattah.mohamed@feng.bu.edu.eg)

ABSTRACT Visible light communication (VLC) is a relatively new wireless communication technology that allows for high data rate transfer. Because of its capability to enable high-speed transmission and eliminate inter-symbol interference, orthogonal frequency division multiplexing (OFDM) is widely employed in VLC. Peak to average power ratio (PAPR) is an issue that impacts the effectiveness of OFDM systems, particularly in VLC systems, because the signal is distorted by the nonlinearity of light-emitting diodes (LEDs). The proposed method Long Short Term Memory-Autoencoder (LSTM-AE) uses an autoencoder as well as an LSTM to learn a compact representation of an input, allowing the model to handle variable length input sequences as well as predict or produce variable length output sequences. This study compares the suggested model with various PAPR reduction strategies to demonstrate that it offers a superior improvement in PAPR reduction of the transmitted signal while maintaining BER. Also, this model provides a flexible compromisation between PAPR and BER.

INDEX TERMS Autoencoder, BER, CCDF, deep learning, LSTM, OFDM, PAPR, RNN, VLC.

I. INTRODUCTION

VLC is frequently utilized because it is a more interesting alternative to the current radio frequency (RF) technology, which has a very limited bandwidth. VLC has a very wide scale bandwidth, is license-free, has low-cost front end devices, and so on [1]. OFDM is often used in RF systems, however it requires to be modified for VLC applications. To modulate the intensity of the LED in a VLC system, the transmitted signal must be unipolar [2]. In addition, the optical signal that is received must have real value in order for the photodetector to reconstruct it [3]. There are two popular methods for meeting these criteria.

The first method is DC-biased Optical OFDM (DCO-OFDM), in order to produce a real-valued signal, an Inverse Fast Fourier Transform (IFFT) is employed after the input is initially restricted to have Hermitian symmetry, and finally a DC-bias is applied to give a positive signal to the LED [4], [5]. The second method is Asymmetric Clipped Optical OFDM (ACO-OFDM), which is primarily used to reduce power waste caused by adding DC-bias to increase energy efficiency [6], [7]. ACO-OFDM sends the signal on the odd subcarriers, utilizing only half of the available bandwidth [8].

However, a high peak to average power ratio (PAPR) is an obvious disadvantage, particularly in ACO-OFDM systems. To lower high PAPR, a Selective Mapping (SLM) [9], a Partial Transmit Sequence (PTS) [10], a genetic algorithm [11], an upper clipping scheme [12], a semi-definite relaxation approach [13] are used. Deep learning can give a new solution to handle this problem because of the vast quantity of data generated during the real functioning of the equipment. Deep learning [14] has been extensively researched in several communication systems, including the encoding and decoding issue [15]. This approach can enhance data throughput, transmission distance, and lighting uniformity in complicated channels. Simultaneously, it can reduce the impact of noise interference and LED nonlinearity on system performance metrics such as SNR and BER. To estimate the channel characteristic, Generative Adversarial Networks [16] are used. The autoencoder network is expanded in the OFDM scheme in [17] and [18]. According to the research, the deep learning approach outperforms the present technology in terms of BER performance in the complicated channel. To simplify the complexity of the active constellation scheme, the authors

The associate editor coordinating the review of this manuscript and approving it for publication was Barbara Masini.

of [19], [20] introduced a neural network (NN), followed by Clipping and Filtering (CF). The authors provide an autoencoder (AE) approach for PAPR reduction while reducing BER deterioration in [21]. To overcome the high PAPR issue with certain types of OFDM signal, the authors of [22], [23] proposed a deep NN paired with Selective Mapping (SLM).

In this paper, we utilize a LSTM-AE model to solve the high PAPR problem while maintaining the BER. The model includes encoding, decoding and the communication channel.

A novel PAPR reduction strategy is this paper's primary contribution which employs a deep LSTM-AE architecture in a VLC DCO-OFDM system. Also, we added a hermetian symmetry and IFFT customized layers in the model structure to train it on a real VLC DCO-OFDM system. LSTM-AE is fed with the constellation symbols and trained adaptably to reduce PAPR while maintaining BER. From the perspective of the complementary cumulative distribution function (CCDF), we compare the performance of the proposed strategy to that of existing PAPR reduction techniques.

The rest of this paper is structured as follows: In section II, Problem definition is introduced. In section III, LSTM-AE structure is demonstrated. In section IV, VLC system model with LSTM-AE is mentioned. The simulation results for the suggested algorithm in the AWGN channel are provided in section V in terms of the CCDF of PAPR and BER. Finally, section VI provides a conclusion and future work for this paper.

II. PROBLEM DEFINITION

The output of a VLC-OFDM system is a superposition of numerous sub-carriers. When the phases of these carriers are the same, the instantaneous power of some outputs may increase dramatically and become significantly greater than the system's mean power. This is also known as a high PAPR [24]. One of the most critical issues with the VLC-OFDM system is high PAPR. If the peak power is excessively high, the LED's linear region may be exceeded. This causes non-linear distortion, which alters the signal spectrum's superposition, leading in performance deterioration. If no steps are taken to lower the high PAPR, the VLC-OFDM system's practical uses may be severely limited.

We assume that the input to our encoder after serial to parallel and M-QAM modulation is $r = [r_1, r_2, \ldots r_N]^T$. To obtain a real signal following the 2N-IFFT operation, the encoded symbols $f(r_{k(k\in[1,N])})$ are then required to be Hermitian symmetric. As illustrated in the following expression, Hermitian symmetry is [25]:

$$S = [f(r_1), f(r_2), \ldots f(r_k), f(r_k)^*, \ldots f(r_2)^*, f(r_1)^*]^T \quad (1)$$

where S is the new vector created following Hermitian symmetry, and (*) is the vector's complex conjugate. In the time domain, the positive real DCO-OFDM symbols $s = [s_1, s_2, \ldots s_{2N}]^T$ are produced after DC bias procedure for VLC transmission.

Equation (2) describes the PAPR definition.

$$PAPR\{S\} = \frac{\max\limits_{1\le k\le 2N} s_k^2}{mean(|s_k^2|)} \quad (2)$$

III. LSTM-AE STRUCTURE

A. AUTOENCODER (AE)

An autoencoder is a kind of artificial neural network that is used to unsupervisedly learn data encodings. An autoencoder's objective is to train the network to capture the most important parts of the input data in order to learn a lower-dimensional form (encoding) for a higher-dimensional data, which is frequently used for dimensionality reduction. AE, which is often used for denoising damaged data, is ideally adapted to dealing with non-linear distortions like high PAPR. As a result, a deep autoencoder model is trained in this research to address the PAPR issue in the VLC DCO-OFDM system.

AE has numerous hidden representation layers [26]. The most interesting characteristic of AE is that the features of each hidden layer are learnt automatically from the input data rather than being constructed manually. As a result, AE has received a lot of attention in recent years, and it is used in a variety of wireless communication applications such as channel coding, channel compensation, and modulation recognition [27].

The standard AE architecture comprises of three components [28]:

- Encoder: A component that compresses the input data into an encoded form that is frequently many orders of magnitude less than the input data.
- Bottleneck: A component that is the most crucial component of the network since it includes the compressed knowledge representations.
- Decoder: This component aids the network in decompressing knowledge representations and reconstructing the data from its encoded state. After then, the result is compared with a ground truth.

Where r is the input, $f(r)$ is the encoder, $g(r)$ is the decoder, and $\tilde{r}$ is the reconstruction of the original input r. Overall, the architecture of the autoencoder is presented in Fig. 1.

The proposed model employs an AE learning system based on a type of Recurrent Neural Network (RNN) called LSTM.

LSTMs were specifically developed to address the issue of long-term reliance. They don't have to do alot of work to recall information for extended periods of time [29]. Also, LSTM-AE allows the model to accommodate variable length input sequences as well as predict or produce varied length output sequences [30].

B. LSTM

Fig. 2 depicts the construction of the LSTM cell. They actually don't differ all that much from other neural networks, as it turns out. The four components of an LSTM—forget gate layer (FGL), input gate layer (IGL), cell state, and output layer—interact in a unique fashion [31]. There are expressed related equations.

$$f_t = \sigma(W_f.[h_{t-1}, X_t] + b_f) \quad (3)$$
$$i_t = \sigma(W_i.[h_{t-1}, X_t] + b_i) \quad (4)$$
$$\tilde{C}_t = tanh(W_C.[h_{t-1}, X_t] + b_C) \quad (5)$$
$$C_t = f_t * C_{t-1} + i_t * \tilde{C}_t \quad (6)$$

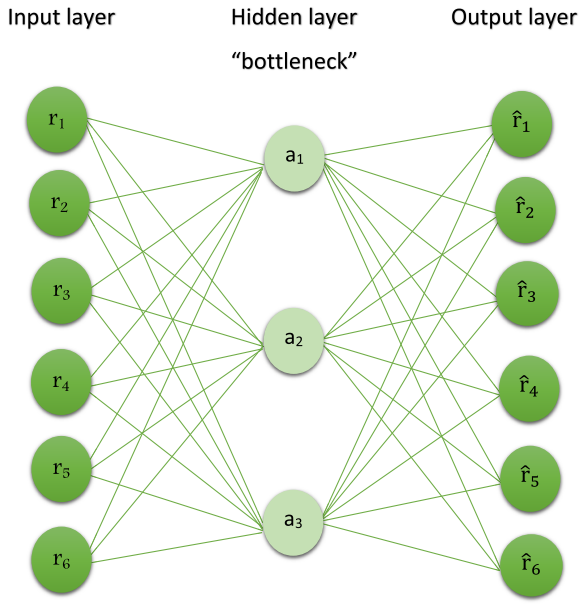

FIGURE 1. Architecture of autoencoder.

$$O_t = \sigma(W_o.[h_{t-1}, X_t] + b_o) \tag{7}$$

$$h_t = O_t * tanh(C_t) \tag{8}$$

where σ represents the sigmoid function, which may be used for transferring a real integer to the range (0,1). FGL creates a vector of 0 and 1 values in (3). Our current cell state, C_t, specifies what we will output. The following step is to choose the new data that will be kept in the cell state. (4) determines which values will be updated, and a tanh layer produces a vector of new candidate values $\tilde{C}_t$ that will be added to the state in (5). The previous cell state C_{t-1} then needs to be updated to the new cell state C_t. To ignore the elements we elected to disregard previously, we multiply C_{t-1} by f_t. According to the regulations, (6) scales each state value, and the output C_t is the filtered version of the current cell state output. (7) (8) decide what we are going to output. X_t and h_t are current input and output vectors, respectively. $W_f, b_f, W_i, b_i, W_C, b_C, W_o, b_o$ are all parameters that are learnt and obtained through the neural network training.

At the encoder, the LSTM cell takes the r vector as its input where $X_t = r$ and produces a bottleneck vector a at the last layer of the encoder where $h_t = a$. At the decoder, the LSTM cell takes the a vector as its input and produces a vector $\tilde{r}$ at the last layer of decoder which represents the output vector.

C. PROPOSED LSTM-AE ARCHITECTURE

In this model, an encoder LSTM model sequentially reads the input sequence. After reading in the whole input sequence, the hidden state or output of this model reflects an internal learned representation of the full input sequence as a fixed-length vector. This vector is then passed to the decoder model, which interprets it when each step in the output sequence is executed.

The proposed LSTM-AE learning system is depicted in Fig. 3. Input of this model is a complex symbols, so to deal with this problem we expand a third dimension to concatenate

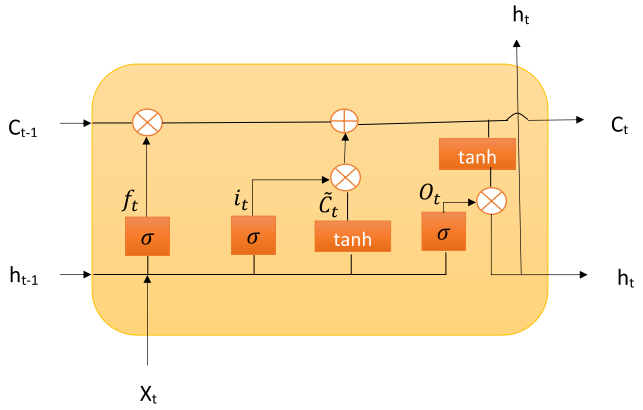

FIGURE 2. LSTM cell structure.

real and imaginary parts of each symbol.LSTM can handle whole data sequences. Because of the model's ability to memorize long-term observation sequences, we use LSTM for recovering and denoising OFDM time series data in the VLC system.

At the encoder, input symbol transmitted through N=256 subcarriers is firstly passed through a Permute layer to convert them to a 256 timesteps then the output is passed through 3 LSTM layers, where each layer is followed by a batch normalization layer. The first LSTM layer has 8 units which means that each timestep consists of 8 feature values which provide 4 alternative symbols. The second LSTM layer has 4 units which means that each timestep consists of 4 feature values which select 2 best symbols that minimize the loss function. The third LSTM layer has 2 units which means that each timestep consists of 2 feature values which select the best symbol that minimizes the loss function. At the end of the encoder we permute the output again to retrieve the original shape of input data. At the decoder, the received symbol is permuted then passed through 2 LSTM and batch normalization layers to recover the encoded data then the output is passed through a fully connected layer with a LeakyReLU activation function to select the best symbols that minimize the total loss function. At the end of the decoder we permute the output again to retrieve the original shape of received data.

D. TRAINING OF THE LSTM-AE NETWORK

The network in our potential methodology is trained to decrease PAPR while limiting BER degradation. As a result, two unique objectives must be considered. First, the model must be able to recover the transmitted signals from the received signals in such a way that the system's BER does not degrade. Second, the model must provide a transmission signal with a low PAPR. We show how the model's suitable loss function may be used to propose a solution for attaining both goals at the same time. The network training procedure is broken into two steps:

1) The parameters of the encoder and decoder are chosen at random. In the loss function, there is simply BER performance. Furthermore, the network has not a channel model. The encoder's output corresponds perfectly to the decoder's input.

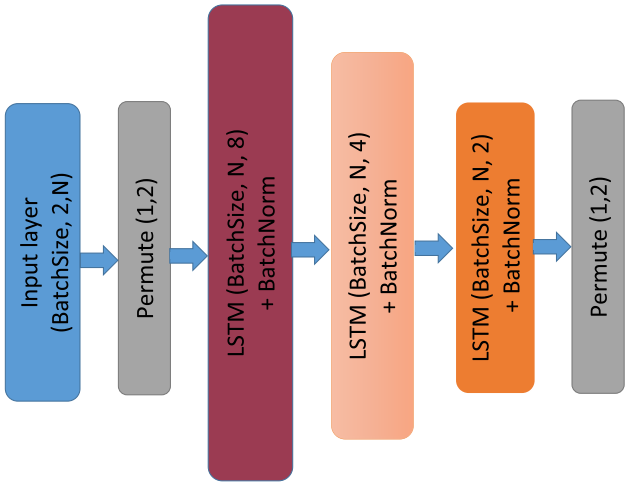

(a) LSTM encoder.

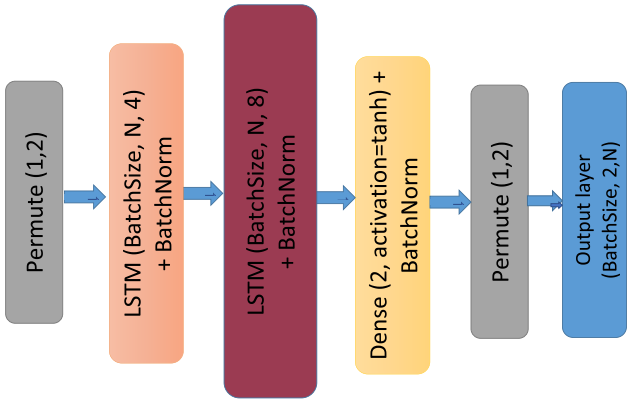

(b) LSTM decoder.

FIGURE 3. LSTM-AE architecture.

2) As the initial values, use the parameters that were learned in Step 1. The loss function is made up of both the BER and the PAPR performance. The proportion of PAPR performance in the loss function is determined by the hyperparameter λ.

Besides, there is a hermetian symmetry layer, IFFT layer after the encoder to simulate the original system during signal transmission while minimizing the PAPR. Also, an Optical channel layer composed of both AWGN and VLC channel noise between the encoder and the decoder is implemented as shown in Fig. 4.

We consider an independently and identically distributed input data sequence consisting of symbol r_k referring to M-bit data, where k represents the index of the symbol and r denotes to the vector of r_k and the reconstructed symbol at the receiver, $\tilde{r}$. can be written as follows in (9):

$$\tilde{r} = g(FFT(h^{-1}(H(IFFT(h(f(r;\theta_f)))) + AWGN))) \quad (9)$$

Mean square error (MSE) is represented as (L_1) in (10):

$$L_1(r,\tilde{r}) = \|r - \tilde{r}\|_2 \quad (10)$$

PAPR loss (L_2) is represented in (11):

$$L_2(r) = PAPR\{IFFT(h(f(r;\theta_f)))\} \quad (11)$$

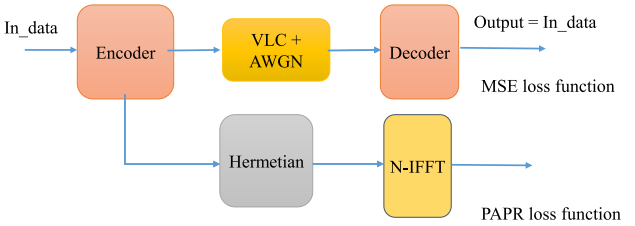

FIGURE 4. Training the LSTM-AE model.

Total loss (L) is represented in (12):

$$L(r,\tilde{r}) = L_1(r,\tilde{r}) + \lambda L_2(r) \quad (12)$$

where $f(.;\theta_f)$ and $g(.;\theta_g)$ are the parametric representation of the encoder and decoder, respectively. h is a hermetian symmetry function, h^{-1} is an inverse of hermetian symmetry, IFFT is the Inverse of Fast Fourier Transform, FFT is the Fast Fourier Transform, AWGN is the Additive White Gaussian Noise, and H is the response of VLC channel.

Through the training, θ_f and θ_g, i.e., the weight and bias of the autoencoder are found such that autoencoder can minimize total loss function.

IV. VLC SYSTEM MODEL WITH LSTM-AE

After training process we can use the trained autoencoder as an inline block to optimize the BER and PAPR losses as shown in Fig. 5 and we can select the appropriate hyperparameter λ according to the application or the study case that focus more on BER or PAPR loss.

In VLC system, bit stream is converted from serial to parallel then mapped to symbols using Quadrature Amplitude Modulation (QAM). The trained encoder selects the best QAM symbols that minimize the loss function. Hermetian symmetry is applied on the symbols then they are modulated on orthogonal subcarriers. This is accomplished through the use of IFFT to get real valued symbols. During channel transmission, orthogonality is maintained. This is performed by prefixing the OFDM frame to be delivered with a cyclic prefix. The cyclic prefix is constructed from the frame's L last samples, which are copied and placed at the beginning of the frame.

It must be greater in length than the channel impulse response. After adding cyclic prefix, symbols are converted from parallel to serial then they are converted to analog signal. Before sending the signal to LED, a DC bias is added to the signal to avoid clipping through LED. Transmitted signal is received through a photo detector like a photodiode then remove the added DC bias at the transmitter. Convert the analog signal to digital signal then convert it from serial to parallel. Strip the added cyclic prefix at the transmitter from the received data. Demodulation of the received data by using FFT and inverse Hermetian symmetry to get the complex symbols. The trained decoder is applied to the received encoded symbols to recover them. Then the complex symbols are demodulated and converted to serial to get the original bit stream.

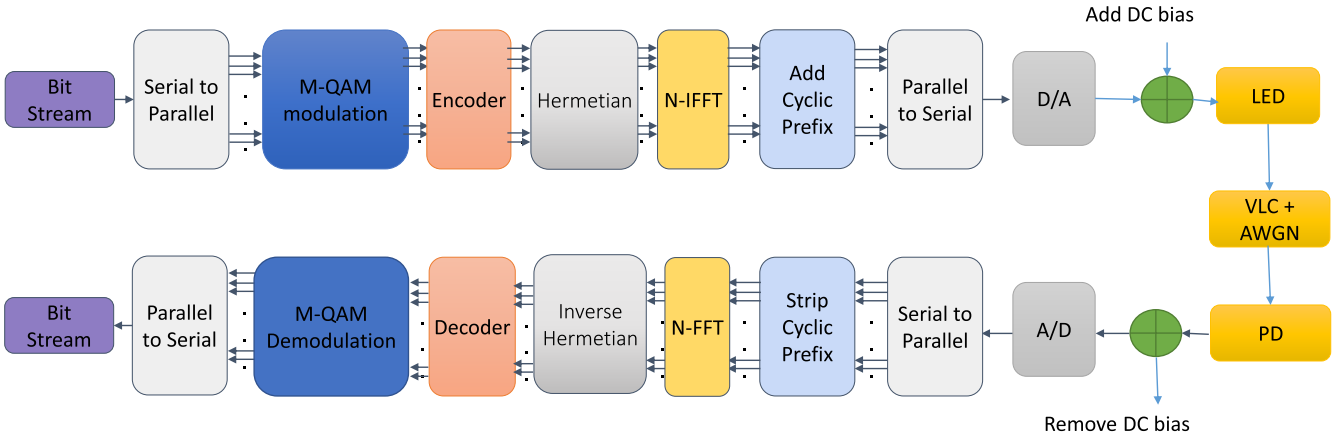

FIGURE 5. VLC system model with LSTM autoencoder structure.

TABLE 1. Simulation parameters.

Parameter	Value
Modulation scheme	16QAM
Number of subcarriers	256
Over sampling rate	4
Cyclic prefix length	100
Channel model	VLC + AWGN
SNR range	0 to 40 dB
Number of training samples	10000
Number of test samples	1000
Optimizer	Adam
Learning rate	0.001
Number of epochs	200
Batch size	512
Room (length, width, height)	10*10*5 m^3
Height of transmitter	1 m
Center luminous intensity	0.73 cd
Minimum LED current	10 mA
Maximum LED current	2 A
Receiver Half angle (FOV)	70 (deg)
Responsivity of photodiode	1 A/W

TABLE 2. LSTM-AE proposed structure.

Layer (type)	Output Shape	Param #
Encoder		
Permute_1	(512, 256, 2)	0
cu_dnnlstm_1	(512, 256, 8)	384
BatchNorm_1	(512, 256, 8)	32
cu_dnnlstm_2	(512, 256, 4)	224
BatchNorm_2	(512, 256, 4)	16
cu_dnnlstm_3	(512, 256, 2)	64
BatchNorm_3	(512, 256, 2)	8
Permute_2	(512, 2, 256)	0
Decoder		
Permute_3	(512, 256, 2)	0
cu_dnnlstm_4	(512, 256, 4)	128
BatchNorm_4	(512, 256, 4)	16
cu_dnnlstm_5	(512, 256, 8)	448
BatchNorm_5	(512, 256, 8)	32
Dense(tanh)	(512, 256, 2)	18
BatchNorm_6	(512, 256, 2)	8
Permute_4	(512, 2, 256)	0

V. SIMULATION RESULTS AND DISCUSSION

In this part, we use the simulation parameters indicated in table 1 to simulate the performance of our suggested approach.

Also, the complete structure of the proposed LSTM-AE is represented in Table 2

PAPR and BER for OFDM VLC system is simulated using Python, Tensorflow and Keras. Fig. 6 indicates the relation between the CCDF and PAPR for conventional OFDM and LSTM-AE with different values of λ. At CCDF $= 10^{-3}$, the conventional OFDM has a PAPR value $= 14$ dB, the proposed autoencoder model has a PAPR value $= 9.8$ dB at $\lambda = 0.5$, a PAPR value $= 9.9$ dB at $\lambda = 0.4$, a PAPR value $= 10.3$ dB at $\lambda = 0.3$, a PAPR value $= 11.3$ dB at $\lambda = 0.2$, a PAPR value $= 13$ dB at $\lambda = 0.1$, and a PAPR value $= 13.9$ dB at $\lambda = 0.01$. We conclude that the proposed autoencoder model has lower PAPR value while increasing the value of hyperparameter λ. But, we note that increasing hyperparameter λ more than 0.3 not imply big difference between the results of PAPR values. The proposed autoencoder has a PAPR value less than the original OFDM of 3.7 dB at $\lambda = 0.3$.

As shown in Fig. 7, we compare the proposed autoencoder at $\lambda = 0.3$ with the Dense-AE that is proposed in [21] at $\lambda = 0.3$, the exponential wavelet OFDM (exp-DWT) proposed in [32] and a clipping technique of clipping ratio 10% with respect to CCDF and PAPR values. At CCDF $= 10^{-3}$, the proposed LSTM-AE has a PAPR value $= 10.3$ dB, the Dense-AE has a PAPR value $= 13.4$ dB, the exp-DWT technique has a PAPR value $= 3.3$ dB and the clipping technique has a PAPR value $= 13$ dB. We found that the exp-DWT outperforms the other techniques with respect to minimum PAPR.

Furthermore, we investigated the BER performance of the proposed autoencoder with different values of hyperparameter λ for the optical channel. As shown in Fig. 8, at BER $=$

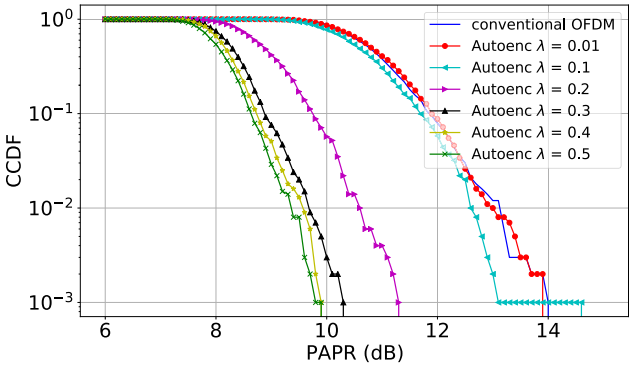

FIGURE 6. CCDF of the PAPR values of proposed autoencoder with different lambda values.

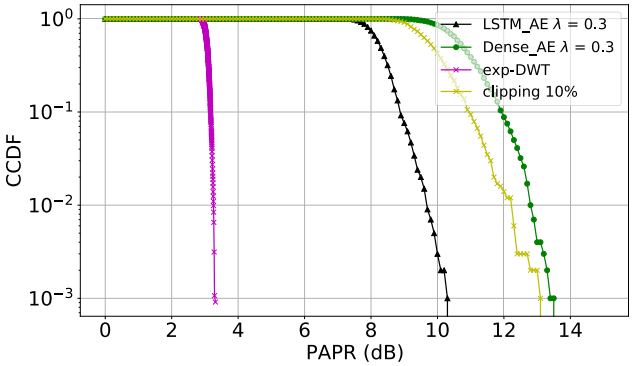

FIGURE 7. CCDF of the PAPR values of proposed autoencoder and different PAPR reduction techniques.

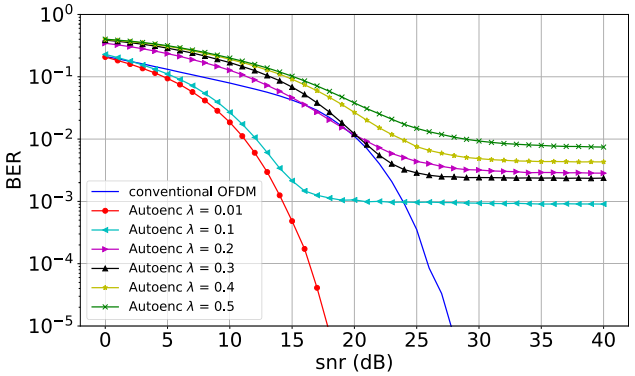

FIGURE 8. BER for the proposed autoencoder at different values of lambda.

10^{-2} the conventional OFDM has SNR value = 20 dB while the proposed LSTM-AE of $\lambda = 0.01$ has SNR value = 11 dB, $\lambda = 0.1$ has SNR value = 12 dB, $\lambda = 0.2$ has SNR value = 20 dB, $\lambda = 0.3$ has SNR value = 20 dB, $\lambda = 0.4$ has SNR value = 23.5 dB, and $\lambda = 0.5$ has SNR value = 29 dB. We conclude that the proposed LSTM-AE model has lower BER value while decreasing the value of hyperparameter λ.

Also, we compare the proposed LSTM-AE at $\lambda = 0.3$ with the Dense-AE at $\lambda = 0.3$, the exp-DWT and the clipping technique of clipping ratio 10% in comparison to BER and SNR values. At SNR = 30 dB, the proposed LSTM-AE has BER $= 3 * 10^{-3}$, the Dense-AE has BER $= 3 * 10^{-1}$, the exp-DWT has BER $= 3 * 10^{-2}$ and the clipping technique has BER $= 6 * 10^{-2}$. We found that the proposed LSTM-AE

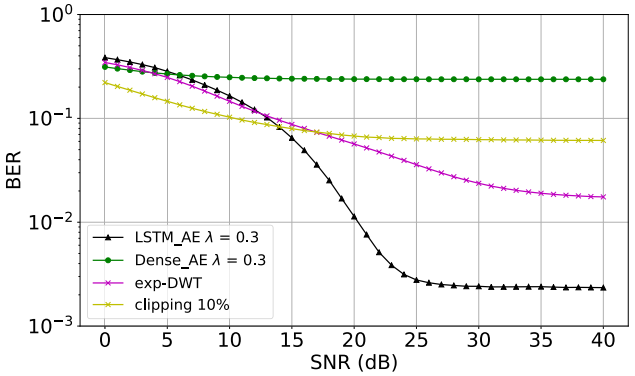

FIGURE 9. BER for the proposed autoencoder and different PAPR reduction techniques.

at $\lambda = 0.3$ outperforms the other techniques in terms of BER, as shown in Fig. 9.

The complexity of the proposed scheme is considered and compared to the Dense-AE model in terms of processing time and number of parameters. We computed the processing time of the proposed model and Dense-AE model by running the algorithms 100 times and taking the average of the total processing time. The processing time of the proposed model is 3.7 s while the processing time of the Dense-AE is 2.5 s. The total number of parameters used in LSTM-AE model is 1378 while the total number of parameters used in Dense-AE model is 1839616.

VI. CONCLUSION AND FUTURE WORK

A LSTM-AE is a suggested deep learning model for PAPR reduction in OFDM system. This model has many remarkable features that are beneficial to VLC system. It deals with variable input sequential data, provides a flexible compromising between PAPR and BER through specifying the appropriate hyperparameter λ. We demonstrated through simulations that our suggested model outperforms traditional schemes in terms of both PAPR and BER. An important extension of this work is the notion of building a faster training method for larger OFDM systems with more subcarriers and greater modulation order.

REFERENCES

[1] T. Komine and M. Nakagawa, "Fundamental analysis for visible-light communication system using LED lights," *IEEE Trans. Consum. Electron.*, vol. 50, no. 1, pp. 100–107, Feb. 2004.

[2] A. F. Aziz, O. A. M. Aly, and U. S. Mohammed, "High efficiency modulation technique for visible light communication (VLC)," in *Proc. 36th Nat. Radio Sci. Conf. (NRSC)*, Apr. 2019, pp. 100–107.

[3] J. Lian, Z. Vatansever, M. Noshad, and M. Brandt-Pearce, "Indoor visible light communications, networking, and applications," *J. Phys., Photon.*, vol. 1, no. 1, Jan. 2019, Art. no. 012001.

[4] J. Armstrong, "OFDM for optical communications," *J. Lightw. Technol.*, vol. 27, no. 3, pp. 189–204, Feb. 1, 2009.

[5] X. Li, R. Mardling, and J. Armstrong, "Channel capacity of IM/DD optical communication systems and of ACO-OFDM," in *Proc. IEEE Int. Conf. Commun.*, Jun. 2007, pp. 2128–2133.

[6] J. Armstrong and A. J. Lowery, "Power efficient optical OFDM," *Electron. Lett.*, vol. 42, no. 6, p. 370, 2006.

[7] J. Armstrong and B. Schmidt, "Comparison of asymmetrically clipped optical OFDM and DC-biased optical OFDM in AWGN," *IEEE Commun. Lett.*, vol. 12, no. 5, pp. 343–345, May 2008.

[8] A. J. Lowery, "Comparisons of spectrally-enhanced asymmetrically-clipped optical OFDM systems," *Opt. Exp.*, vol. 24, no. 4, pp. 3950–3966, Feb. 2016.
[9] H. Lu, Y. Hong, L.-K. Chen, and J. Wang, "On the study of the relation between linear/nonlinear PAPR reduction and transmission performance for OFDM-based VLC systems," *Opt. Exp.*, vol. 26, no. 11, pp. 13891–13901, May 2018.
[10] Z. E. Ankarali, S. I. Hussain, M. Abdallah, K. Qaraqe, H. Arslan, and H. Haas, "Clipping noise mitigation using partial transmit sequence for optical OFDM systems," in *Proc. 3rd Int. Workshop Opt. Wireless Commun. (IWOW)*, Sep. 2014, pp. 80–84.
[11] H.-L. Hung and Y.-F. Huang, "Peak-to-average power ratio reduction in orthogonal frequency division multiplexing system using differential evolution-based partial transmit sequences scheme," *IET Commun.*, vol. 6, no. 11, pp. 1483–1488, 2012.
[12] W. Xu, M. Wu, H. Zhang, X. You, and C. Zhao, "ACO-OFDM-Specified recoverable upper clipping with efficient detection for optical wireless communications," *IEEE Photon. J.*, vol. 6, no. 5, pp. 1–17, Oct. 2014.
[13] H. Zhang, Y. Yuan, and W. Xu, "PAPR reduction for DCO-OFDM visible light communications via semidefinite relaxation," *IEEE Photon. Technol. Lett.*, vol. 26, no. 17, pp. 1718–1721, Sep. 1, 2014.
[14] F. Musumeci, C. Rottondi, A. Nag, I. Macaluso, D. Zibar, M. Ruffini, and M. Tornatore, "An overview on application of machine learning techniques in optical networks," *IEEE Commun. Surveys Tuts.*, vol. 21, no. 2, pp. 1383–1408, 2nd Quart., 2019.
[15] T. J. O'Shea and J. Hoydis, "An introduction to deep learning for the physical layer," 2017, *arXiv:1702.00832*.
[16] T. J. Oshea, T. Roy, N. West, and B. C. Hilburn, "Physical layer communications system design over-the-air using adversarial networks," in *Proc. 26th Eur. Signal Process. Conf. (EUSIPCO)*, Sep. 2018, pp. 529–532.
[17] J. Schmidhuber, "Deep learning in neural networks: An overview," *Neural Netw.*, vol. 61, pp. 85–117, Oct. 2014.
[18] M. Kim, W. Lee, and D.-H. Cho, "A novel PAPR reduction scheme for OFDM system based on deep learning," *IEEE Commun. Lett.*, vol. 22, no. 3, pp. 510–513, Mar. 2018.
[19] I. Sohn, "A low complexity PAPR reduction scheme for OFDM systems via neural networks," *IEEE Commun. Lett.*, vol. 18, no. 2, pp. 225–228, Feb. 2014.
[20] I. Sohn and S. C. Kim, "Neural network based simplified clipping and filtering technique for PAPR reduction of OFDM signals," *IEEE Commun. Lett.*, vol. 19, no. 8, pp. 1438–1441, Aug. 2015.
[21] L. Shi, X. Zhang, W. Wang, Z. Wang, A. Vladimirescu, Y. Zhang, and J. Wang, "PAPR reduction based on deep autoencoder for VLC DCO-OFDM system," in *Proc. IEEE Int. Symp. Broadband Multimedia Syst. Broadcast. (BMSB)*, Jun. 2019, pp. 1–4.
[22] L. Hao, D. Wang, Y. Tao, W. Cheng, J. Li, and Z. Liu, "The extended SLM combined autoencoder of the PAPR reduction scheme in DCO-OFDM systems," *Appl. Sci.*, vol. 9, no. 5, p. 852, Feb. 2019.
[23] L. Hao, D. Wang, W. Cheng, J. Li, and A. Ma, "Performance enhancement of ACO-OFDM-based VLC systems using a hybrid autoencoder scheme," *Opt. Commun.*, vol. 442, pp. 110–116, Jul. 2019.
[24] K. Srinivasarao, "Peak-to-average power reduction in MIMO-OFDM systems using sub-optimal algorithm," *Int. J. Distrib. Parallel Syst.*, vol. 3, no. 3, pp. 261–273, May 2012.
[25] H. Lin and P. Siohan, "OFDM/OQAM with Hermitian symmetry: Design and performance for baseband communication," in *Proc. IEEE Int. Conf. Commun.*, May 2008, pp. 652–656.
[26] Y. Bengio, L. Yao, G. Alain, and P. Vincent, "Generalized denoising auto-encoders as generative models," in *Proc. Adv. Neural Inf. Process. Syst.*, vol. 26, 2013, pp. 1–9.
[27] G. E. Hinton and R. R. Salakhutdinov, "Reducing the dimensionality of data with neural networks," *Science*, vol. 313, no. 5786, pp. 504–507, 2006.
[28] D. Bank, N. Koenigstein, and R. Giryes, "Autoencoders," 2020, *arXiv:2003.05991*.
[29] A. Sherstinsky, "Fundamentals of recurrent neural network (RNN) and long short-term memory (LSTM) network," *Phys. D, Nonlinear Phenomena*, vol. 404, Mar. 2020, Art. no. 132306.
[30] T. Ergen and S. S. Kozat, "Online training of LSTM networks in distributed systems for variable length data sequences," *IEEE Trans. Neural Netw. Learn. Syst.*, vol. 29, no. 10, pp. 5159–5165, Oct. 2018.
[31] S. Hochreiter and J. Schmidhuber, "Long short-term memory," *Neural Comput.*, vol. 9, no. 8, pp. 1735–1780, 1997.
[32] A. Mohamed, A. S. T. E. Dein, and R. S. Saad, "PAPR reduction of wavelet-OFDM signals using exponential companding in visible light communications," in *Proc. 15th Int. Conf. Comput. Eng. Syst. (ICCES)*, Dec. 2020, pp. 1–5.

ABDELFATAH MOHAMED received the B.Sc. degree in electrical engineering from the Faculty of Engineering at Shoubra, Benha University, Egypt, in 2016. He is currently a Teacher Assistant with the Department of Electrical Engineering, Faculty of Engineering at Shoubra, Benha University. His research interests include VLC, machine learning, the IoT, and smart grid communications.

ADLY S. TAG ELDIEN received the B.Sc., M.Sc., and Ph.D. degrees from Benha University, Egypt, in 1984, 1989, and 1993, respectively. He is currently the Ex-Head of the Network and Information Center, and the Head of Electrical Engineering Department, Faculty of Engineering at Shoubra, Benha University. His research interests include robotics, networks, and mobile communication.

MOSTAFA M. FOUDA (Senior Member, IEEE) received the B.S.E.E. degree (as the Valedictorian) and the M.S.E.E. degree from Benha University, Egypt, and the Ph.D. degree in information sciences from Tohoku University, Japan. He was an Assistant Professor at Tohoku University and a Postdoctoral Research Associate at Tennessee Technological University, Cookeville, TN, USA. He is currently an Assistant Professor with the Department of Electrical and Computer Engineering, Idaho State University, Pocatello, ID, USA. He also holds the position of a Full Professor at Benha University. He has (co)authored more than 120 technical publications. His current research interests include cybersecurity, communication networks, signal processing, wireless mobile communications, smart healthcare, smart grids, AI, and the IoT. He has received several research grants, including NSF-JUNO3 and INL LDRD. He has guest-edited a number of special issues covering various emerging topics in communications, networking, and health analytics. He is also serving on the Editorial Board for the IEEE TRANSACTIONS ON VEHICULAR TECHNOLOGY and IEEE ACCESS.

REHAM S. SAAD received the B.S. degree in electronics and communication engineering, the M.Sc. degree in handover performance optimization for wireless and mobile networks, and the Ph.D. degree in performance analysis of channel estimation techniques for LTE from Benha University, in 2006, 2012, and 2016, respectively. She is currently a Lecturer with the Faculty of Engineering at Shoubra, Benha University. Her research interests include LiFi, small cells, LoRa technology, and mobile communications.